

Numerical Construction of Deformation Field Under Wedge Indentation

Ayob, S. * and Mohd Damanhuri, N. A.

*Faculty of Industrial Sciences and Technology, Universiti Malaysia
Pahang, Malaysia*

E-mail: syafikah7182@gmail.com

** Corresponding author*

Received: 15 January 2020

Accepted: 4 November 2020

ABSTRACT

This research paper presented the construction of the stress distribution in the deformation region under a smooth rigid wedge indenter. The stress components were assumed to satisfy the Mohr-Coulomb yield condition under the plane strain condition. The governing equation for the model was the first order partial differential equation, the stress equilibrium equations. The deformation region was made up of the union of the adjacent elementary boundary value problem and was solved numerically. The region was constructed using Matlab and shows the lip formation on the stress-free surface. The result then compared to analytical solutions. This method is of great interest as it will bring about an increase in efficiency and hence, improvement in industrial productivity. The method is also an alternative for the solution of deformation problems as it is simple and more reliable. This method will consequently improve in designing and developing tools in the related industries and will eventually increase its efficiency.

Keywords: Deformation, granular material, plasticity, wedge indentation.

1. Introduction

Granular materials can be found across a wide range of scales for example, in the kitchen, we have sugar, salt, cereals, in geophysics, we found sand, gravel, as well as, asteroids in astrophysics, (see Harris (2014)). Storage, handling, and processing of granular materials are procedures required in numerous industries and are of interest to various branches of science and technology such as physics, chemistry, mechanics, agriculture, and engineering. The agriculture and food industry are, next to chemical, power, and pharmaceutical industries, the largest producers and users of granular materials. Although the granular is easy to figure, they exhibit complex behaviour. They can't be easily classified as solids, liquid or gases. The equipment for storage and processing of granular materials should meet two necessary conditions, which are predictable and safe operations and high quality of finished products.

A precise knowledge of how they behave under these circumstances is essential for the efficient design and application of related industries. Their behaviour is like a new form state besides those three properties. The mathematical modelling for these materials is very complex due to their mechanical behaviour. Granular materials show both solid and fluid behaviour. The study of rheology properties of granular materials is essential for many industries including mining and mineral processing, agriculture, construction, food processing and pharmaceutical. A precise knowledge of how they behave under these particular circumstances is essential for efficient design and applications for the related industries. For example, when one adds wheat, sugar, grains, cement, or sand and gravels, the fact that all these materials need to be transported and stored, the importance of granular materials become self-evident. Granular materials usually stored in hoppers or bins. For example, agricultural hoppers that contain, for example, grains, can measure up to 20m in diameter and 60m height.

The predictions of the stress distributions and the flow patterns throughout the hopper are exceptionally very important. The stresses can be so significant and the flow pattern can be so complicated which can cause the hoppers to collapse or destroyed. Although there are many industrial applications, this field still requires more accurate scientific analysis to control loss in production, extra labour and inefficient use of capital. In many situations, we need considerable improvement in the flow of granular materials. For example, discharging large quantities of grain from a hopper or discharging grain into the extruder. It is essential to know how these materials react as they are released and begin to flow. They are very sensitive to various factors such as shape and size of the particles, wall roughness, flow rate and the coupling with the interstitial fluid,

etc. Due to their complexity, it is shown that modelling granular materials would need ideas from both solid and fluid mechanics fields. For example, the phenomenon of dilatancy that was postulated by Reynolds ?. Many of the existing theories for flowing granular materials use this observation to associate the applied stress to the volume fraction and the velocity, Goddard (1999), Massoudi and Mehrabadi (2001). They are also crucial for geological processes where landslides, erosion, and on a related field but much larger scale, plate tectonics determine much of the morphology of the earth, Jaeger et al. (1996).

The numerical method approximates the solution of many technical problems, such as in designing embankments, retaining walls, tunnels, and all other related industries. In this paper, the problem of the indentation of granular material by a smooth rigid wedge was considered. For simplicity, the weight of the material was neglected. The solution to the same problem in a perfectly plastic material was obtained by Hill et al. (1947). The authors considered a pseudo-steady plastic flow in which the slip line field, the stresses, and the velocity changed but retained its shape. By closely following their solution, Shield (1953) proposed a solution to the normal indentation of soil by a smooth rigid wedge under the plane strain condition on the assumption that the stresses satisfy the Mohr-Coulomb yield criteria. Then, in 1998, Tordesillas and Shi (1998) proposed an analytical solution to the plane strain indentation problem by a smooth rigid wedge of a double shearing model for dilatant materials. The authors generalized the formulation given by Butterfield and Harkness (1972) and Mehrabadi and Cowin (1978) and compared their solution with the materials obeying incompressible double shearing theory and Mohr-Coulomb associated flow rule.

We aimed to construct the stress distribution field in the deformation region under a smooth rigid wedge by using the numerical approximation method. The stress field in the whole deformation region is constructed when the wedge $B'AB$ is penetrated into the surface of granular material $E'E$ as in Figure 1. The stress field in deformation region is constructed from the contact surface AB to the free surface. The whole deformation region obtained by then being constructed using Matlab. The stress field is established using the characteristic slip line method, in which the stress is define from one region to the next, starting from the wedge punch surface to the raised surface. There are some boundary value problems involved in determining the stress field under the punch. Several distinct types of construction of boundary value problems are seems to occur repeatedly in the same problem but in different part of plastic region, Hill and Selvadurai (2005). Damanhuri (2017) proposed a numerical solution method that were frequently used in metal plasticity to the double slip and double spin model developed by Harris and Grekova (2005). The

author assumed that the deformational response to loading is planar and the flow occurs at each point in the deformation region of two simultaneous shears. A smooth rigid flat punch considers the indentation problem. The extension of the numerical method for the double slip and double spin model was given by Ayob and Mohd Damanhuri (2019) by a wedge punch. From the numerical approximation obtained in Damanhuri (2017) and Ayob and Mohd Damanhuri (2019), the method will be applied to the whole deformation region in the problem of the indentation by a smooth rigid wedge.

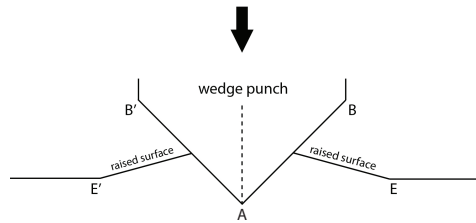


Figure 1: Wedge Indentation.

In this paper, we constructed a numerical method to construct stress distribution in the deformation region by using the Matlab program. In section 2, the basic equation for stress will be discussed, while in section 3, we summarize the numerical method for the basic construction of the stress characteristics field. The numerical construction of the stress field is presented in section 4. Furthermore, the discussion and conclusion of the study are presented in section 5.

2. The Stress Equation

The stress equilibrium equations were given by

$$\frac{\partial \sigma_x}{\partial x} + \frac{\partial \sigma_{xy}}{\partial y} = 0 \quad (1)$$

$$\frac{\partial \sigma_{xy}}{\partial x} + \frac{\partial \sigma_y}{\partial y} = 0 \quad (2)$$

with Mohr Coulomb yield criterion

$$\tau = c - \sigma_n \tan \phi \quad (3)$$

where c is the cohesion and ϕ represents the friction angle. In a plastic state, the stresses can be expressed as follows:

$$\begin{aligned}\sigma_x &= -p + q \cos 2\psi \\ \sigma_{xy} &= q \sin 2\psi \\ \sigma_y &= -p - q \cos 2\psi\end{aligned}\tag{4}$$

where p and q are the mean stress and the maximum shearing stress, defined by

$$p = -\frac{1}{2}(\sigma_x + \sigma_y), q = \frac{1}{2}(\sigma_x - \sigma_y).\tag{5}$$

From equations (1) and (2), the stress characteristics directions are defined by

$$\frac{dy}{dx} = \tan \left[\left(\psi - \left(\frac{\pi + 2\phi}{4} \right) \right) \right] \text{ are called } \alpha\text{-characteristic line}\tag{6}$$

$$\frac{dy}{dx} = \tan \left[\left(\psi + \left(\frac{\pi + 2\phi}{4} \right) \right) \right] \text{ are called } \beta\text{-characteristic line.}\tag{7}$$

These two characteristic lines represent two failure planes on which the failure criterion is satisfied. By substituting equations (4) into the Equation (1) and (2), the governing stress equations for p and ψ were define by

$$\frac{\partial p}{\partial L_\alpha} \cos \phi + 2q \frac{\partial \psi}{\partial L_\alpha} = 0\tag{8}$$

$$-\frac{\partial p}{\partial L_\beta} \cos \phi + 2q \frac{\partial \psi}{\partial L_\beta} = 0\tag{9}$$

where ψ was the gradient and $\frac{\partial}{\partial L_\alpha}, \frac{\partial}{\partial L_\beta}$ were the directional derivatives along α - and β -characteristic line respectively. Since these equations were hyperbolic, the solution are determined by using the method of characteristics Hill (1998).

3. Numerical Approximation Method

As the wedge indenter is penetrated the surface of the granular material, the deformation will occur, and hence, the stress distribution field in the whole plastic deformation region was constructed. Figure 2 shows the pattern of the failure lines after the penetration. The displaced materials were squeezed out towards the surface, which forms a lip, namely the raised surface. Following Hill (1998) and Shield (1953), the surface of the raised surface was considered as a straight line. The triangular region OPQ and PRS were the regions of constant

stresses. Region PQR was centered field region of angle θ_2 and the raised surface PS made an angle θ_1 with the free surface TE. The length of the raised surface PS is denoted by r , the distance of the origin T from line PS was denoted by k , the height of P from the free surface TS was denoted by h and the depth of the penetration was denoted by d . Thus, in terms of d , θ_1 , and θ_2 , we had

$$r = \frac{d}{e^{-\theta_2 \tan \phi} \tan\left(\frac{\pi-2\phi}{4}\right) \cos \theta_2 - \sin \theta_1} \tag{10}$$

$$h = \frac{d \sin \theta_1}{e^{-\theta_2 \tan \phi} \tan\left(\frac{\pi-2\phi}{4}\right) \cos \theta_2 - \sin \theta_1}. \tag{11}$$

3.1 Elementary Boundary Value Problem

Several different types of characteristic line construction are found to occur repeatedly in the solution of deformation problems, occurring in the same problem but different parts of the plastic deformation region. In the next section, we discuss the four elementary value problems used in the solving process.

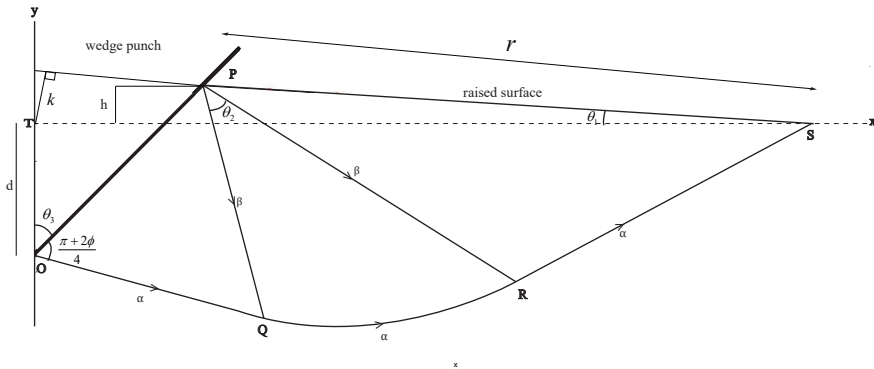


Figure 2: Deformation region under the wedge.

3.1.1 First Elementary Boundary Value Problem

The deformation field can be defined when the intersecting characteristic lines are known. Supposing that two intersecting characteristic lines α and β

were known, then the stress distribution field within the region in Figure 3 was uniquely determined.

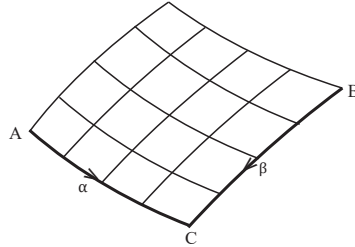


Figure 3: The intersection of two characteristic lines is known.

3.1.2 Second Elementary Boundary Value Problem

Suppose that all stresses components are known on the non-characteristic line AB, as in Figure 4. The example of a non-characteristic line, in this case, is the contact surface. The determination of α , β -characteristic curve depends upon the value of ψ on AB. For the theory of characteristics, the known condition on AB is sufficient to determine the stress field in plastic region ABC.

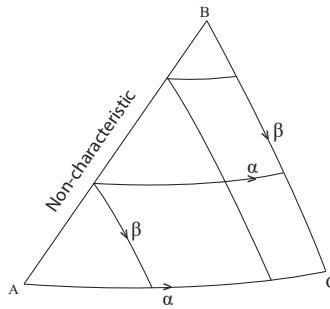


Figure 4: All stress components (x, y, p, ψ) on a non-characteristic line are known.

3.1.3 Third Elementary Boundary Value Problem

This type of elementary boundary value problem is a special case of the first elementary boundary value problem. It is also known as the centred fan. This type of elementary boundary value problem occurs when one of the characteristics, for example, α -characteristic BE in Figure 5 degenerates to a single point and the characteristics form a central region. The point B is known as a singular point. At singular point B , the stress variables p and ψ are discontinuous.

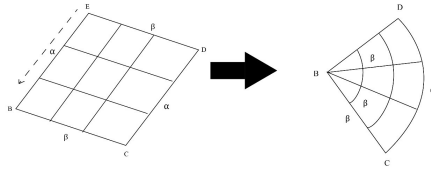


Figure 5: Centered fan region

3.1.4 Fourth Elementary Boundary Value Problem

If the characteristic of AC is given and the value of ψ is specified on a non-characteristic line AB in Figure 6, then the stress field in ABC is determined uniquely. The example of a non-characteristic line in this case is the raised surface.

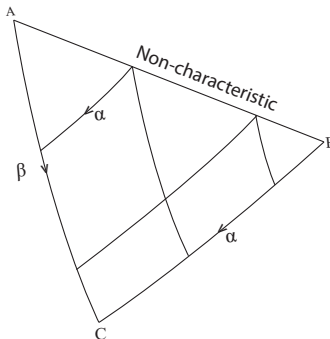


Figure 6: One characteristic curve known together with a curve along which the value of ψ is known.

3.2 The Solution Method

Let the α -characteristic line pass through n_0n_2 and β -characteristic line pass through n_1n_2 . The position (x, y) and the stress variables (p, ψ) at n_0, n_1 , and n_2 be denoted by (x_0, y_0, ψ_0, p_0) , (x_1, y_1, ψ_1, p_1) , and (x_2, y_2, ψ_2, p_2) , respectively. The angle between the α - and β -characteristic line and the x -axis is $[\psi - (\frac{\pi+2\phi}{4})]$ and $[\psi + (\frac{\pi+2\phi}{4})]$ respectively as shown in Figure 7. From the Equation (6) and (7), we have,

$$y_0 - y_2 = (x_0 - x_2) \tan \left[\psi_\alpha - \left(\frac{\pi + 2\phi}{4} \right) \right] \text{ at the } \alpha\text{-characteristic line and} \quad (12)$$

$$y_1 - y_2 = (x_1 - x_2) \tan \left[\psi_\beta + \left(\frac{\pi + 2\phi}{4} \right) \right] \text{ at the } \beta\text{-characteristic line} \quad (13)$$

where ψ_α and ψ_β are the values along α - and β - characteristic lines respectively. Then, by solving the equation simultaneously, the approximated solution for Equation (14) and (15) at point $n_2(x_2, y_2, \psi_2, p_2)$ are given by

$$x_2 = \frac{x_1 \tan \left[\psi_\beta + \left(\frac{\pi + 2\phi}{4} \right) \right] - x_0 \tan \left[\psi_\alpha - \left(\frac{\pi + 2\phi}{4} \right) \right] + y_0 - y_1}{\tan \left[\psi_\beta + \left(\frac{\pi + 2\phi}{4} \right) \right] - \tan \left[\psi_\alpha - \left(\frac{\pi + 2\phi}{4} \right) \right]} \quad (14)$$

$$y_2 = \frac{(x_1 - x_0) \tan \left[\psi_\beta + \left(\frac{\pi + 2\phi}{4} \right) \right] \tan \left[\psi_\alpha - \left(\frac{\pi + 2\phi}{4} \right) \right]}{\tan \left[\psi_\beta + \left(\frac{\pi + 2\phi}{4} \right) \right] - \tan \left[\psi_\alpha - \left(\frac{\pi + 2\phi}{4} \right) \right]} + \frac{y_0 \tan \left[\psi_\beta + \left(\frac{\pi + 2\phi}{4} \right) \right] - y_1 \tan \left[\psi_\alpha - \left(\frac{\pi + 2\phi}{4} \right) \right]}{\tan \left[\psi_\beta + \left(\frac{\pi + 2\phi}{4} \right) \right] - \tan \left[\psi_\alpha - \left(\frac{\pi + 2\phi}{4} \right) \right]} \quad (15)$$

where

$$\psi_\alpha = \frac{1}{2}(\psi_0 + \psi_2) \quad (16)$$

$$\psi_\beta = \frac{1}{2}(\psi_1 + \psi_2) \quad (17)$$

at the α -characteristic line n_0n_2 and β -characteristic line n_1n_2 respectively.

From the solution given by Equation (14) and (15), the approximation solution for (ψ_2, p_2) are defined as follows.

Let the length of α - characteristic line n_0n_2 and of β - characteristic line n_1n_2 be represented by ∂L_α and ∂L_β respectively.

$$\partial L_\alpha = L_0^\alpha - L_2^\alpha \text{ at the } \alpha \text{- characteristic line } n_0n_2 \quad (18)$$

$$\partial L_\beta = L_1^\beta - L_2^\beta \text{ at the } \beta \text{ - characteristic line } n_1 n_2. \quad (19)$$

Hence, from the Equations (8) and (9) along the α - and β -characteristic,

$$\frac{\partial p}{\partial L_\alpha} = \frac{p_0 - p_2}{L_0^\alpha - L_2^\alpha}, \frac{\partial p}{\partial L_\beta} = \frac{p_1 - p_2}{L_1^\beta - L_2^\beta}, \frac{\partial \psi}{\partial L_\alpha} = \frac{\psi_0 - \psi_2}{L_0^\alpha - L_2^\alpha}, \frac{\partial \psi}{\partial L_\beta} = \frac{\psi_1 - \psi_2}{L_1^\beta - L_2^\beta} \quad (20)$$

Therefore, stress variables ψ_2 and p_2 are determined by

$$\psi_2 = \frac{(\psi_0 + \psi_2) \cos \phi + 2q_\alpha \psi_0 + 2q_\beta \psi_1}{2q_\alpha + 2q_\beta} \quad (21)$$

$$p_2 = \frac{p_0 \cos \phi + 2q_\alpha (\psi_0 - \psi_2)}{\cos \phi} \quad (22)$$

where

$$q_\alpha = \frac{1}{2}(p_0 + p_2) \sin \phi + c \cos \phi, q_\beta = \frac{1}{2}(p_1 + p_2) \sin \phi + c \cos \phi \quad (23)$$

along the α - and β -characteristics respectively.

In order to find the solution for the coordinates (x, y) and the stress variables (p, ψ) at point $n_2(x_2, y_2, \psi_2, p_2)$, an iterative procedure is required. After the $(m + 1)^{th}$ iteration, the approximation for $(x_2^{(m+1)}, y_2^{(m+1)}, \psi_2^{(m+1)}, p_2^{(m+1)})$ was obtained.

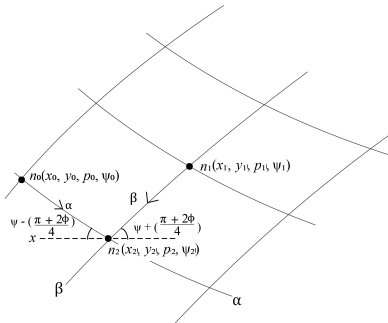


Figure 7: Two intersecting characteristic lines are known

4. The Construction of Stress Distribution in Plastic Region

Due to the symmetrical configuration about the y-axis, we only consider the right half of the field. From the boundary conditions, the deformation region can be divided into three distinct regions as in the following subsections.

4.1 Construction of stress distribution field under the contact surface

The pressure distribution on the contact surface OP in Figure 8 was assumed to be known. The surface OP was divided into $(n - 1)$ equal parts and each point was labeled as $OPQ(m, 1)$ where $m = 1, \dots, n$. The coordinates (x, y) and the stress variables (p, ψ) were given along the contact surface OP. In this surface, by following Hill (1998), we shall assumed the stresses were constant, therefore the solution for p and ψ would give a constant value. The point $OPQ(1,1)$ and $OPQ(2,1)$ were the neighbouring points on the contact surface OP, and the intersection of β -characteristic line that passing through $OPQ(1, 1)$ and the α -characteristic line passed through $OPQ(2, 1)$ is labeled as $OPQ(1, 2)$ as in Figure 8. The coordinates and the stress variables p and ψ of point $OPQ(1, 2)$ could be defined by employing the numerical procedure described in section 3.2. Once point $OPQ(1, 2)$ was constructed, then by considering the next two neighbouring points on the contact surface $OPQ(2, 1)$ and $OPQ(3, 1)$, the point $OPQ(2, 2)$ could be defined. This procedure was repeated until the intersection point $OPQ(1, n)$ was determined. Thus, from the contact surface OP, we constructed the stress distribution field in region OPQ by using Matlab as shown in Figure 8.

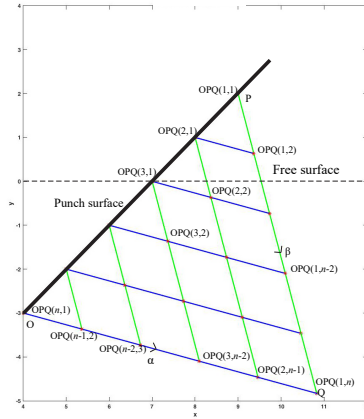


Figure 8: Matlab construction of stress distribution field under the contact surface.

4.2 Construction of centered fan type region

This type of region can be constructed from the extension from the line PQ in subsection 4.1 where point P is called the stress singularity point. In region PQR, there are a family of β -characteristic lines which are straight and all meet at point P, and a family of circles arcs, which is the α -characteristic with angle θ_2 . The stress variables p and ψ were discontinued at P. Let P be divided into n arc and the initial n points at P is denoted by $PQR(m, 1)$ where $m = 1, \dots, n$. All initial points at a singular point P have the same coordinates as the initial point $PQR(1, 1)$ but the value of stress variables p and ψ at each initial point is different. From region PQR, as discussed in subsection 4.1, the coordinate and the stress variable at each point along β -characteristic line PQ are known. Then, the point $PQR(2, 1)$ and neighbouring point $PQR(1, 2)$ was considered. As in Figure 9, a point $PQR(2, 2)$ is the intersection of the α -characteristic line and the β -characteristic line that passing through the point $PQR(1, 2)$ and $PQR(2, 1)$ respectively. Since the coordinates and the stress variables at both points are known, then by applying the procedure method described in subsection 3.2, the solution at point $PQR(2, 2)$ is determined. Then, the next point $PQR(3, 2)$ is considered. As shown in Figure 9, a point $PQR(3, 2)$ was the intersection of α - and the β -characteristic lines passing through point $PQR(2, 2)$ and $PQR(3, 1)$, respectively. By repeating the procedure discussed above, the stress distribution field in the region of PQR was developed.

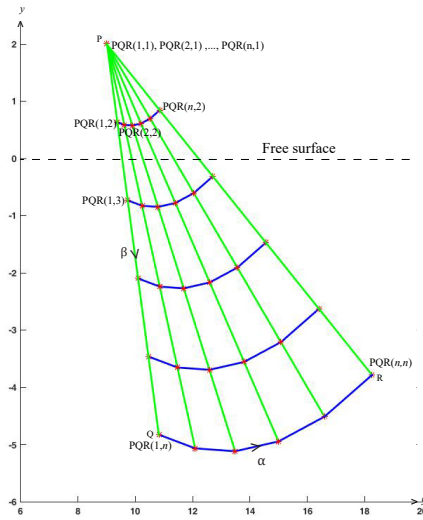


Figure 9: Matlab construction of stress distribution in centered fan type region.

4.3 Construction of deformation region under the free surface

Let PS denote the raised surface that was caused by the punch. The coordinate y and the angle of ψ on PS were known. PR be a known β -characteristic resulting from the centered fan field region PQR in subsection 4.2. Therefore, the coordinates and the stress variables for along PR were also identified. Let PR be divided into $(n - 1)$ equal parts and each point was labeled as PRS(1, m) where where $m = 1, \dots, n$. To construct the stress field in this region, we considered two points PRS(2, 1) on PS and PRS(1, 3) on the known β -characteristic line PR. PRS(2, 2) was the intersection of β -characteristic that passed through PRS(2, 1) and α -characteristic line that passed through point PRS(1, 3). At point PRS(2, 1), the coordinate y and the angle of ψ were known. The x -coordinate and the pressure, p at PRS(2, 1) can be defined by using the equation in subsection 3.2. Now, consider the point PRS(2, 2) where the α -characteristic line that passed through PRS(1, 3) and β -characteristic that passing through PRS(2, 1) intersect. The point PRS(2, 2) can be defined by considering the two neighboring points PRS(2, 1) and PRS(1, 3) using the numerical method described in subsection 3.2. This procedure was repeated until the intersection point PRS(1, n) was obtained. Figure 10 shows the stress field in the deformation region PRS constructed by Matlab.

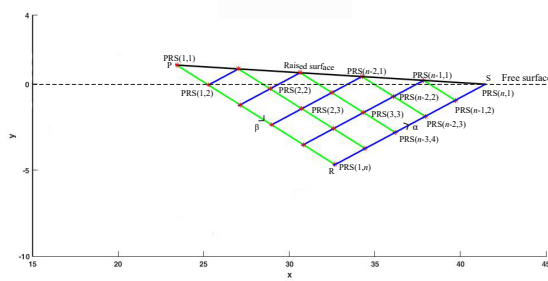


Figure 10: Matlab construction of deformation region under the free surface.

We constructed all three deformation regions and the stress distribution field for the whole deformation region as shown in Figure 11.

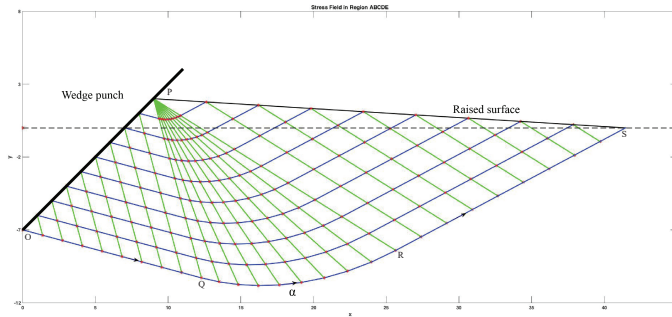


Figure 11: Matlab construction of stress field under wedge.

5. Results and Discussion

The indentation problem by a wedge punch gave the solution for the stress distribution field with semi-angle $\theta_3 = \frac{\pi}{4}$. The internal friction was $\phi = \frac{\pi}{6}$ and the cohesion was $c = 2$. Thus, the computed values of p and ψ in region PQR were compared to the analytical solution given by Tordesillas and Shi (1998) as shown in Figure 12.

The results showed a small difference between the two solutions. As a conclusion, it is fair to say that the numerical method of construction of the

deformation of granular material under wedge punch is simple and more general to be applied. By using this numerical approach, we can define the stress distribution at each point in which will give a better solution.

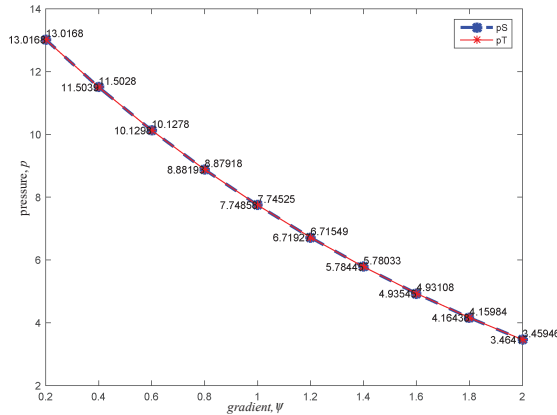


Figure 12: Comparison of the pressure p and angle ψ with Tordesillas's calculation.

Acknowledgement

We are grateful to Universiti Malaysia Pahang for the financial support of this research under UMP internal grant RDU170355.

References

- Antony, S. J., Hoyle, W., Ding, Y., and Ding, Y. (2004). Constitutive modelling of flowing granular materials: A continuum approach. In M. Mehrdad (Eds), *Granular Materials: Fundamentals and Applications* (pp 63–107). doi. 10.1039/9781847550996-00063.
- Ayob, S. and Mohd Damanhuri, N. (2019). Numerical approximation of plane deformation for the indentation of granular material by a smooth rigid wedge punch. *Universal Journal of Mechanical Engineering*, 7(4):166–171.
- Butterfield, R. and Harkness, R. M. (1972). The kinematics of mohr-coulomb materials. *Proceedings of the Roscoe Memorial Symposium: Stress Strain Behaviour of Soils* (ed. Parry, R. H. G.), pages 220–233.

- Damanhuri, N. A. and Ayob, S. (2017). A general numerical approximation of construction of axisymmetric ideal plastic plane deformation of a granular material. *Journal of Physics: Conference Series*, 890(1):012059.
- Damanhuri, N. A. M. (2017). *The numerical approximation to solutions for the double-slip and double-spin model for the deformation and flow of granular materials*. PhD thesis. The University of Manchester, United Kingdom.
- Goddard, J. D. (1999). Granular dilatancy and the plasticity of glassy lubricants. *Industrial and Engineering Chemistry Research*, 38(3):820–822.
- Harris, D. (2014). A hyperbolic augmented elasto-plastic model for pressure-dependent yield. *Acta Mechanica*, 225:2277–2299.
- Harris, D. and Grekova, E. F. (2005). A hyperbolic well-posed model for the flow of granular materials. *Journal of Engineering Mathematics*, 52(1-3):107–135.
- Hill, J. M. and Selvadurai, A. P. (2005). Mathematics and mechanics of granular materials. *Journal of Engineering Mathematics*, 52:1–9.
- Hill, R. (1998). *The mathematical theory of plasticity*. New York: Oxford University Press.
- Hill, R., Lee, E. H., and Tupper, S. J. (1947). The theory of wedge indentation of ductile materials. *Proceeding of the Royal Society of London. Series A, Mathematical, Physical and Engineering Sciences*, 188(1013):273–289.
- Jaeger, H. M., Nagel, S. R., and Behringer, R. P. (1996). Granular solids, liquids, and gases. *Reviews of Modern Physics*, 68:1259–1273.
- Massoudi, M. and Mehrabadi, M. M. (2001). A continuum model for granular materials: Considering dilatancy and the mohr-coulomb criterion. *Acta Mechanica*, 152:121–138.
- Mehrabadi, M. M. and Cowin, S. C. (1978). Initial planar deformation of dilatant granular materials. *Journal of the Mechanics and Physics of Solids*, 26(4):269–284.
- Shield, R. T. (1953). Mixed boundary value problems in soil mechanics. *Quarterly of Applied Mathematics*, 11(1):61–75.
- Tordesillas, A. and Shi, J. (1998). Indentation of a double shearing dilatant granular material by a smooth rigid wedge. *Quarterly Journal of Mechanics and Applied Mathematics*, 51(4):633–646.